Search for high-mass resonances and other exotica at the LHC

John Butler

Boston University

for the ATLAS and CMS collaborations

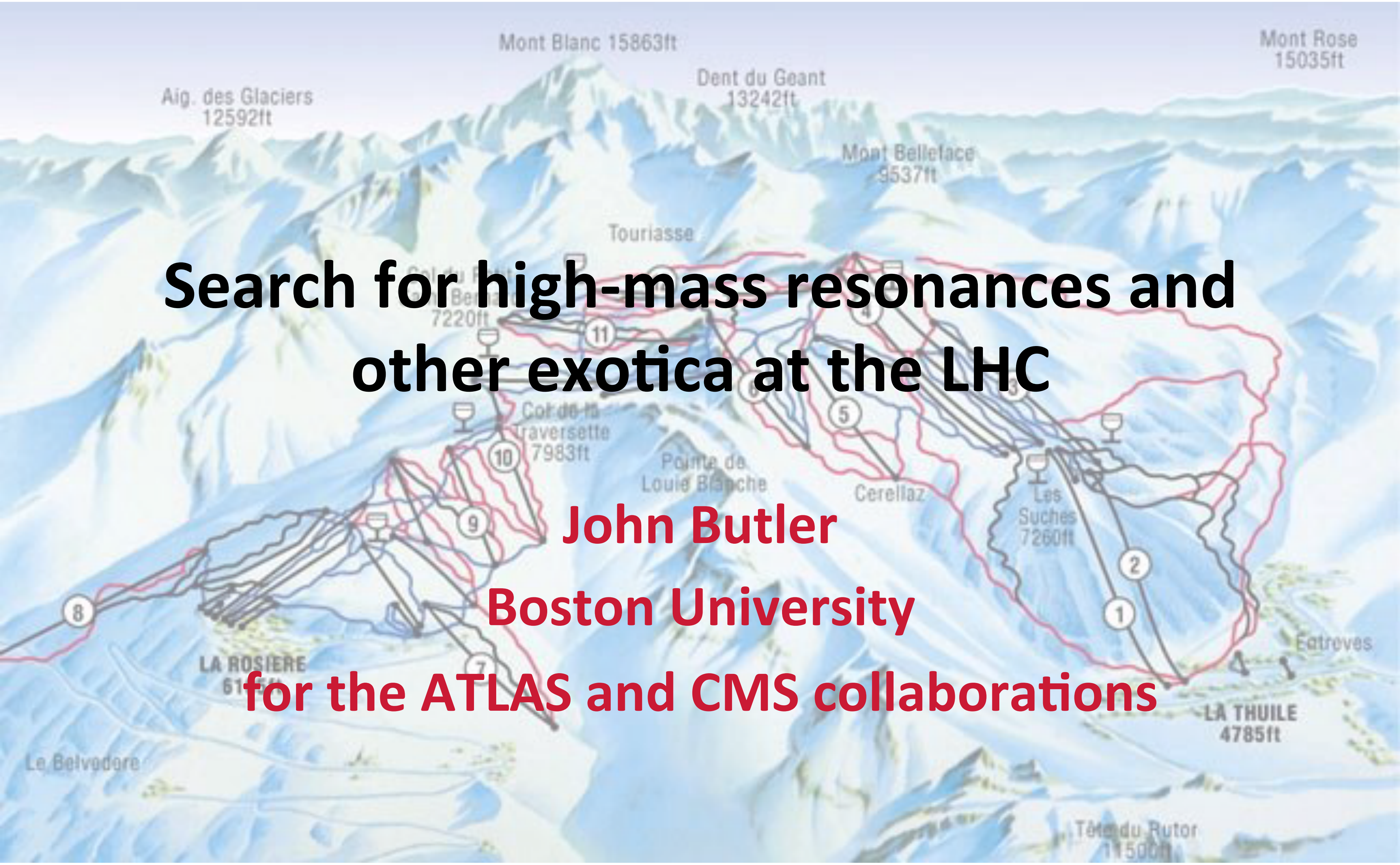

Outline

- Motivation
- Results of ATLAS and CMS searches for
  - Dilepton resonances*#
  - Resonances decaying to lepton + MET#
  - Type III seesaw model heavy leptons*
  - Resonant WZ → 3lν production*
  - Resonant ZZ Production
  - Dijet resonances#
- Summary

*New for Moriond

#Newish (26 Feb 13)

Motivation

- The Standard Model (SM) provides an excellent description of HEP experimental data
  - No major SM-data discrepancies
  - If "Higgs-like" → SM scalar, all SM particles observed
- And yet…the SM leave many questions unanswered
  - Dark matter, # generations, hierarchy problem…
- Numerous Beyond-the-SM (BSM) theories predict new phenomena at the TeV scale that are accessible at the LHC
- Search for BSM resonances on smooth SM backgrounds
  - Focus on a selection of recent results, apologies if your favorite is left out
  - Lepton $l = e, \mu$
  - All limits are quoted at the 95% CL

High-Mass Dilepton Resonances

ATLAS & CMS results @ 8 TeV
Search for heavy narrow dilepton resonances: Z' (SSM, E6), MWT, RS G*…
ATLAS [20 fb^{-1}, CONF-2013-TBA]
CMS [21 fb^{-1}, EXO-2012-061]

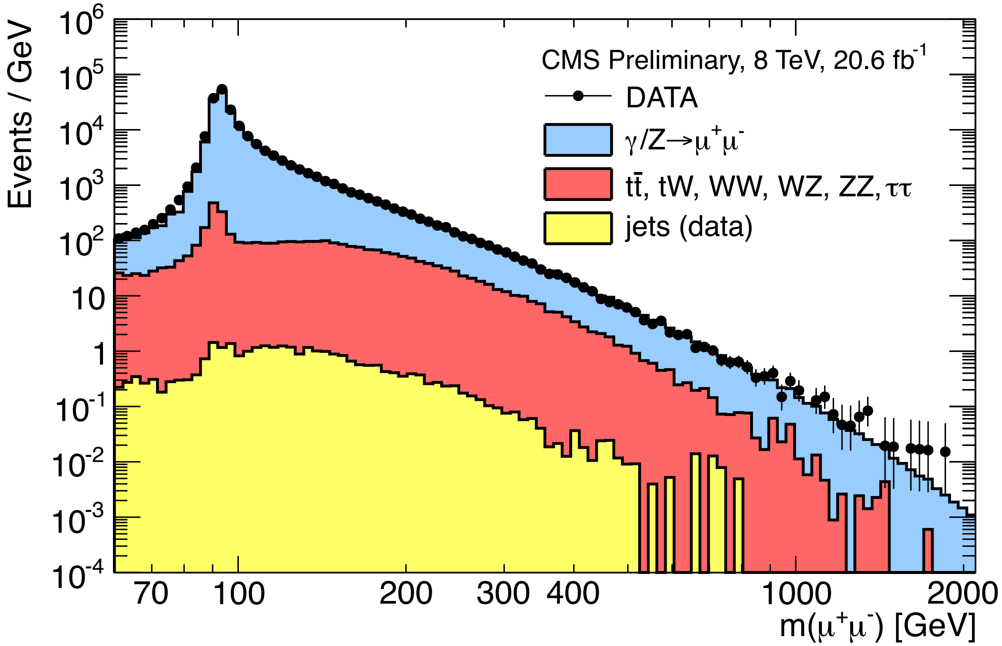

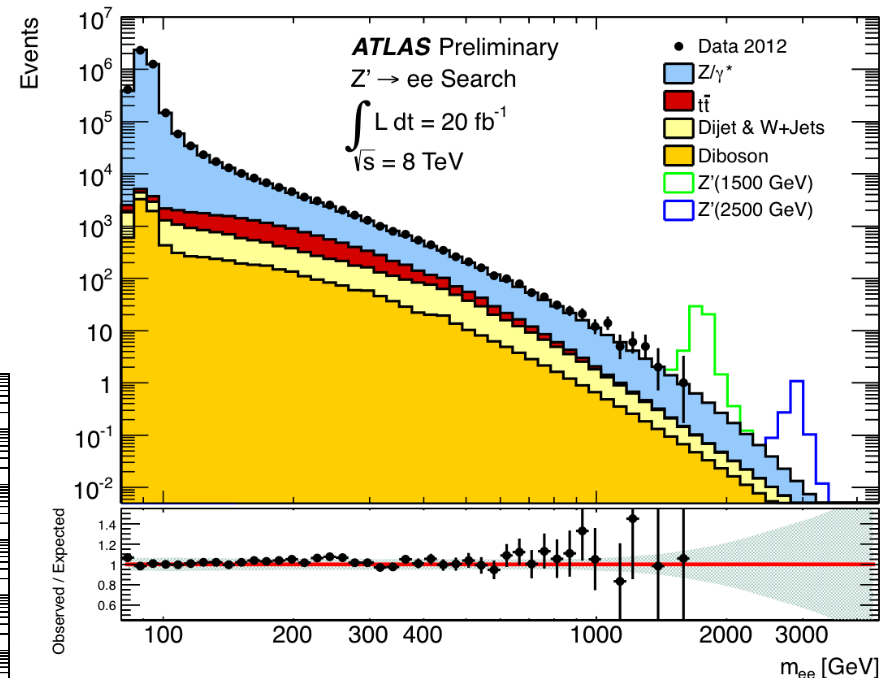

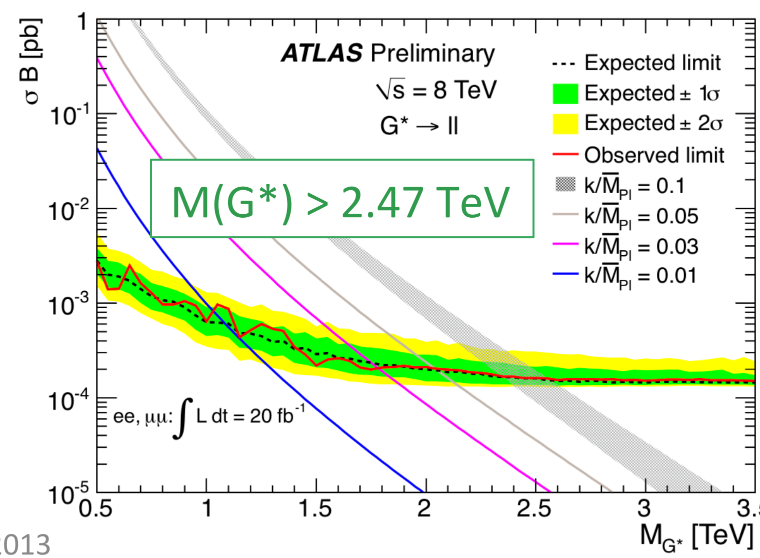

For the benchmark SSM Z' model
m(SSM Z') > 2.96 TeV [CMS]
> 2.86 TeV [ATLAS]

W' → Lepton + MET

Search for heavy resonances decaying to l+MET: W' (SSM, E6), W*, UED…
ATLAS [5 fb^{-1} @ 7 TeV, EPJ C 72:2241]
CMS [20 fb^{-1} @ 8 TeV, EXO-2012-060]

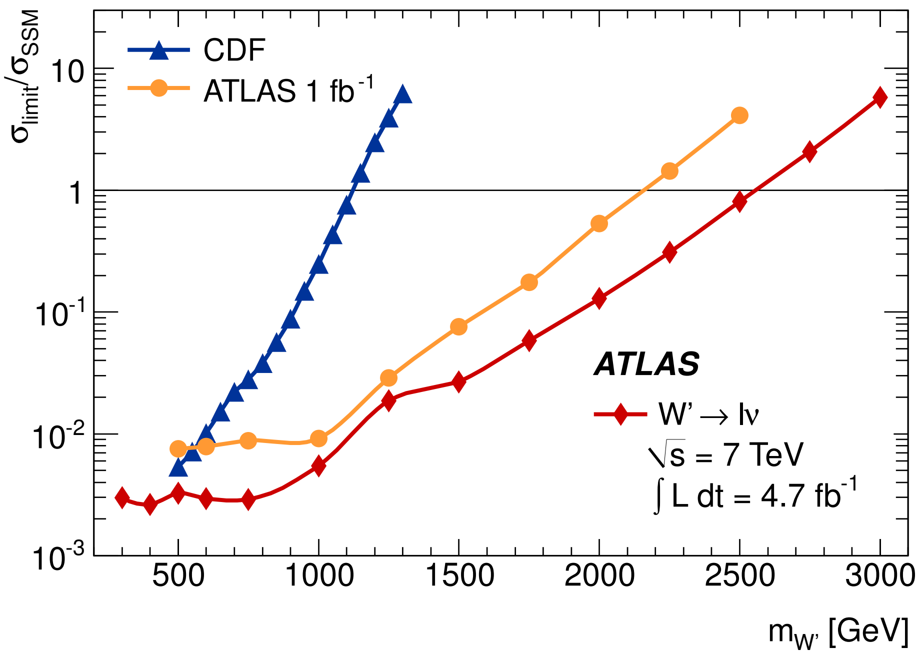

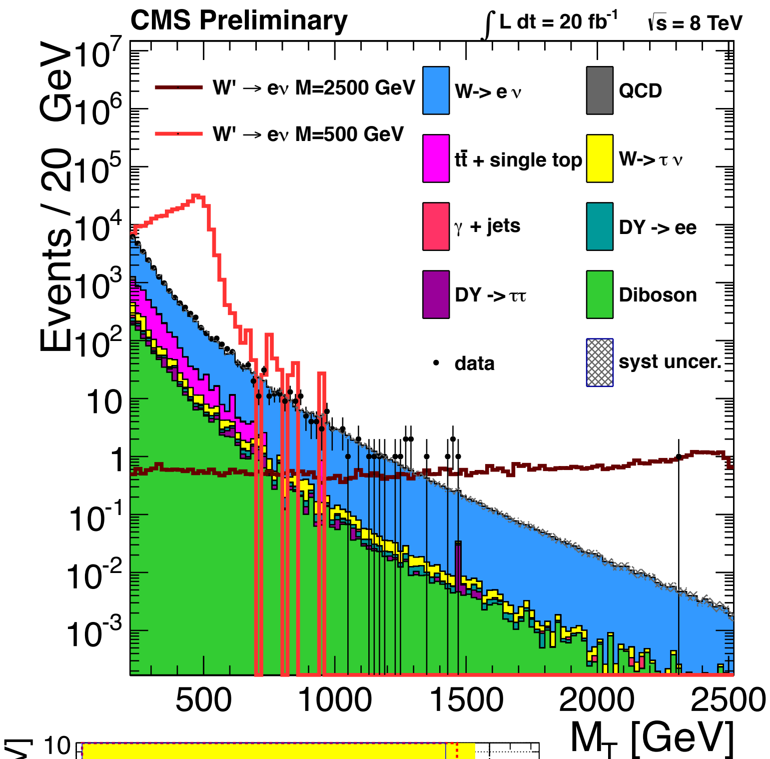

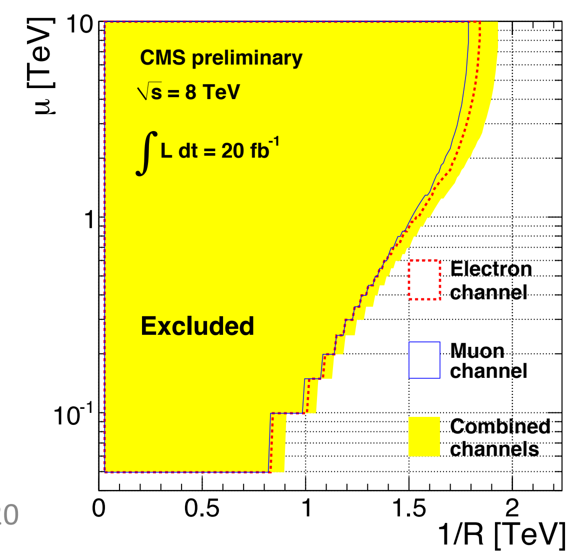

For the benchmark SSM W' model
m(SSM W') > 3.35 TeV [CMS]
> 2.55 TeV [ATLAS]

Type III Seesaw Model Heavy Leptons

Seesaw models generate light masses of neutrinos with addition of massive particles
CMS: $\Sigma^{\pm}\Sigma^{0}$ where $\Sigma^{\pm} \rightarrow W\,\nu$, $\Sigma^{0} \rightarrow W\,l$
CMS [5 fb^{-1} @ 7 TeV, PLB **718**, 348]
ATLAS: $N^{\pm}N^{0}$ where $N^{\pm} \rightarrow Z\,l^{\pm}$, $N^{0} \rightarrow W\,l$
ATLAS [6 fb^{-1} @ 8 TeV, CONF-2013-TBA]

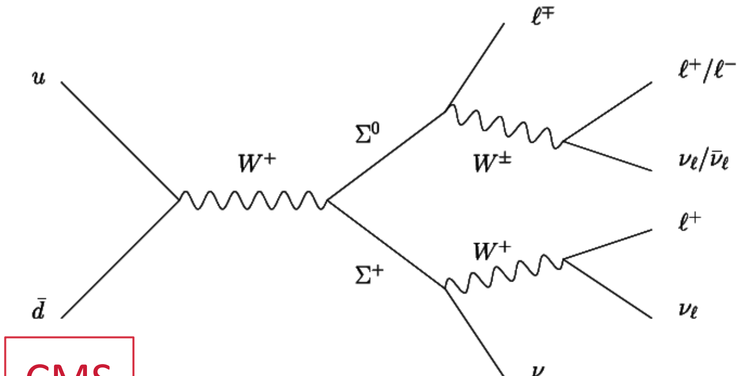

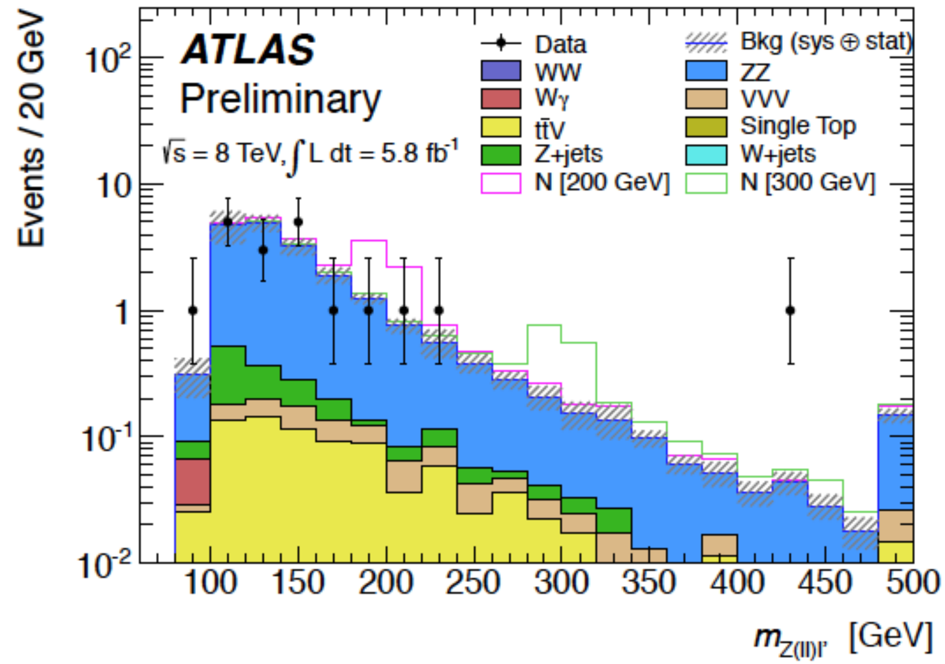

CMS

Scenario	95% CL: $\sigma\mathcal{B}$ (fb)		95% CL: M_{Σ} (GeV)	
	Exp.	Obs.	Exp.	Obs.
FDS	22	20	177	179
μS	13	11	201	211
eS	13	13	202	204

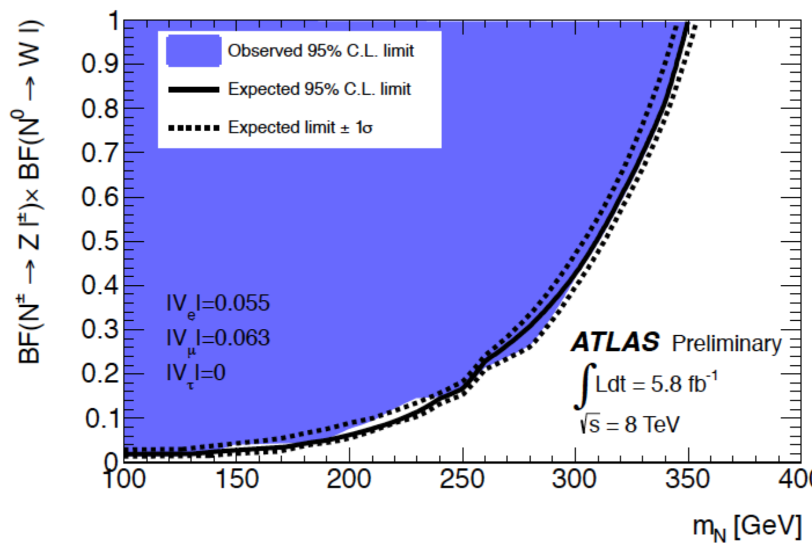

M(N) > 245 GeV [ATLAS]
> 350 GeV for ∏ B = 1.00

Resonant WZ → 3lν Production

BSM mechanisms of EWSB predict diboson resonances: EGM W', LSTC…

CMS [5 fb^{-1} @ 7 TeV, PRL **109**, 141801]

ATLAS [13 fb^{-1} @ 8 TeV, CONF-2013-TBA]

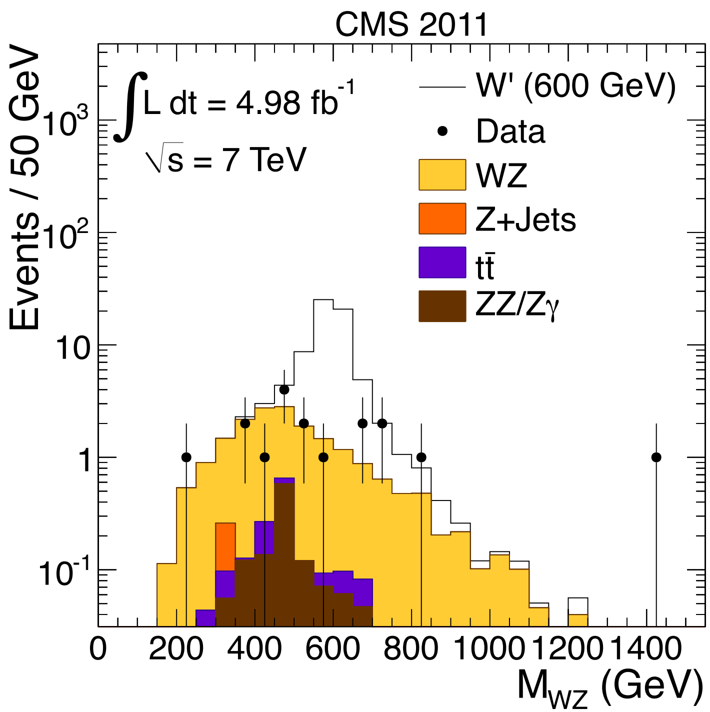

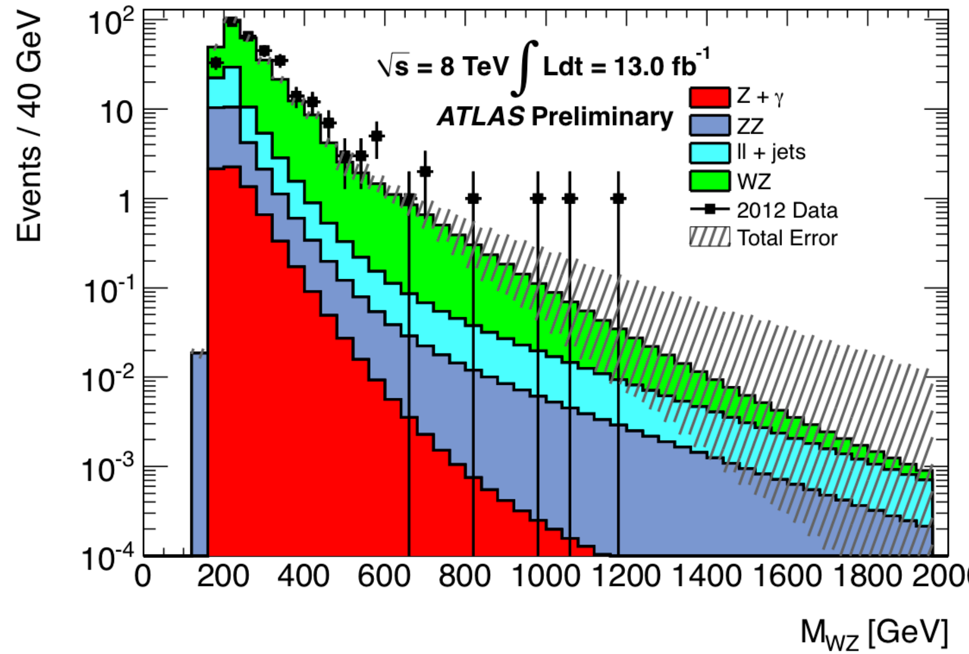

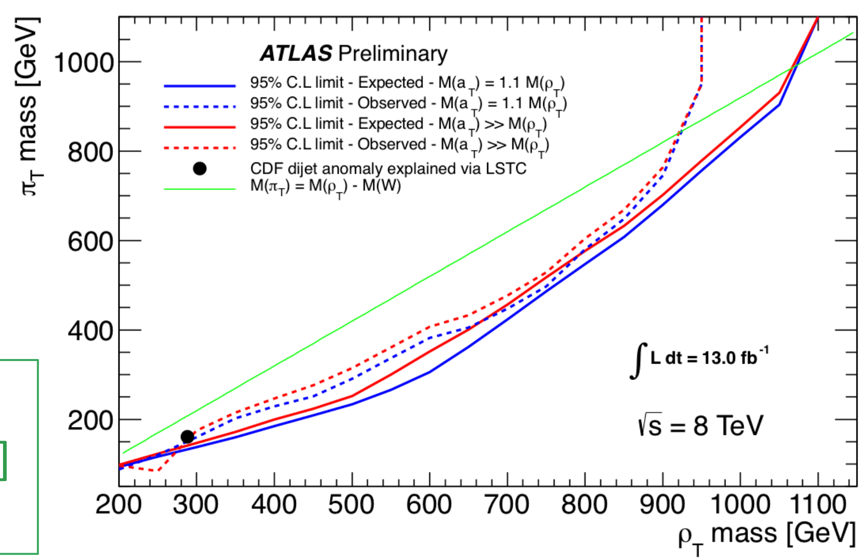

For the benchmark W' model

m(EGM W') > 1.18 (1.30) TeV [ATLAS]

> 1.14 TeV [CMS]

Resonant ZZ Production

Search for G → ZZ where Z→ll, Z→jj
CMS [5 fb^{-1} @ 7 TeV, PLB **718**, 1208]
ATLAS [7 fb^{-1} @ 8 TeV, CONF-2012-150]
For Z→jj, jets can be “resolved” or “merged”

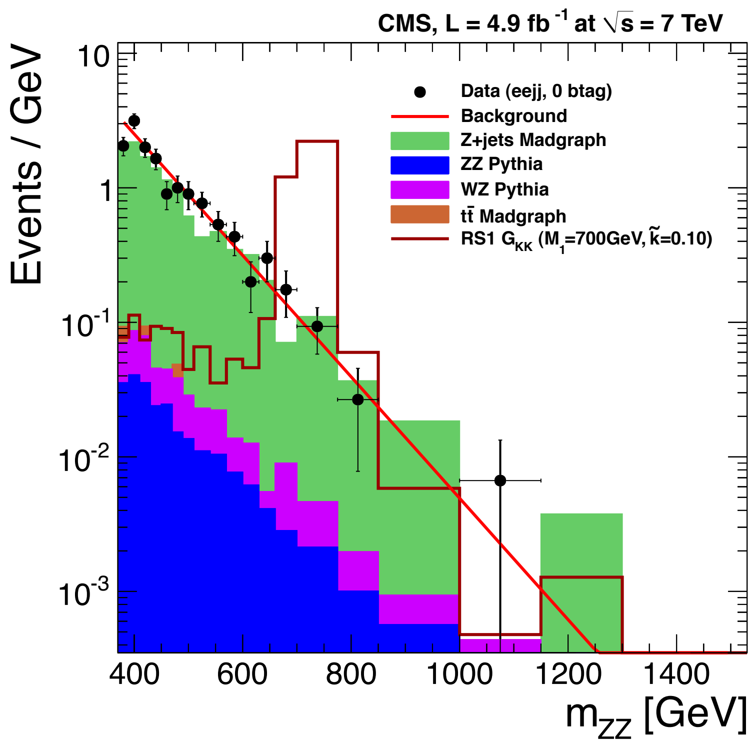

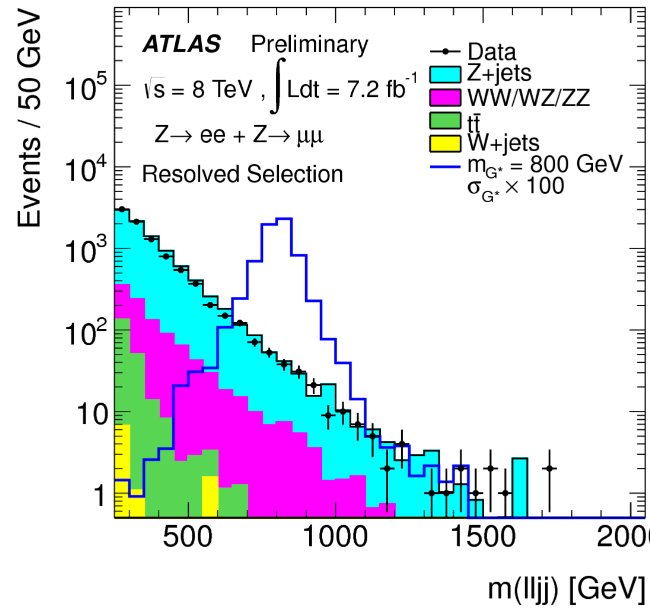

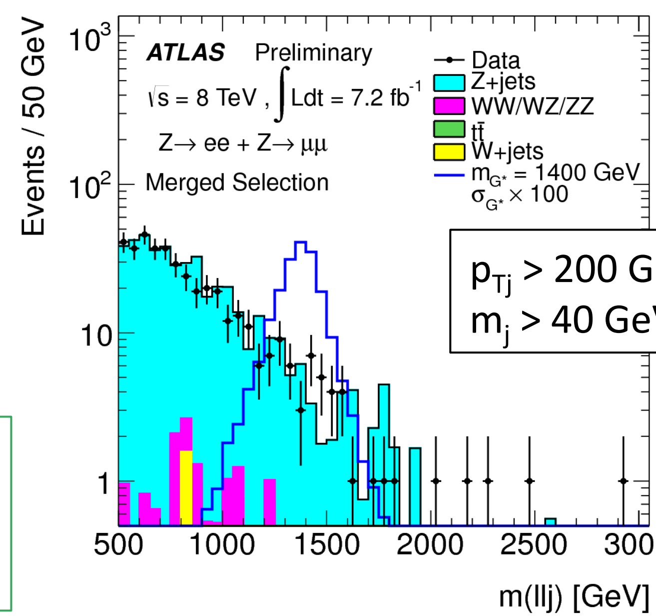

p_{Tj} > 200 GeV
m_j > 40 GeV

For bulk RS gravitons
m > 850 GeV (k/M_{Pl} = 1.00) [ATLAS]
> 610 GeV (k/M_{Pl} = 0.50) [CMS]

Dijet Resonances

ATLAS & CMS results @ 8 TeV. Many BSM dijet resonances predict narrow s-channel resonances: q*, W', Z', RS G…
ATLAS [13 fb^{-1}, CONF-2012-148] and CMS [20 fb^{-1}, EXO-12-059]

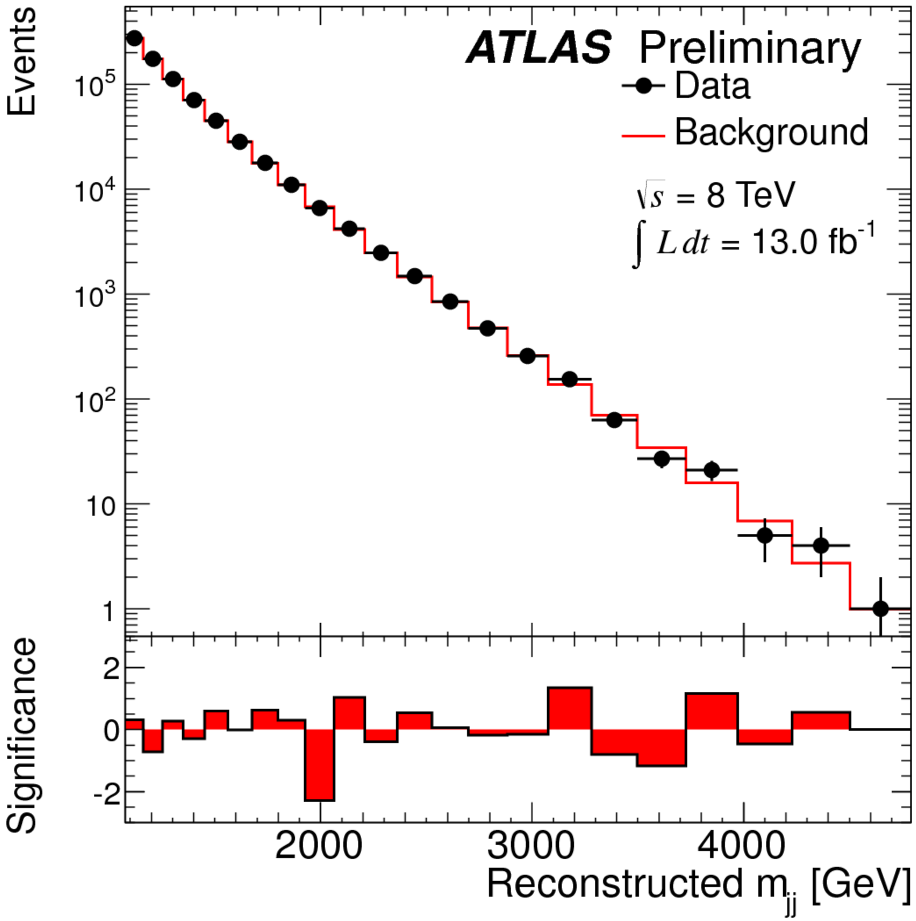

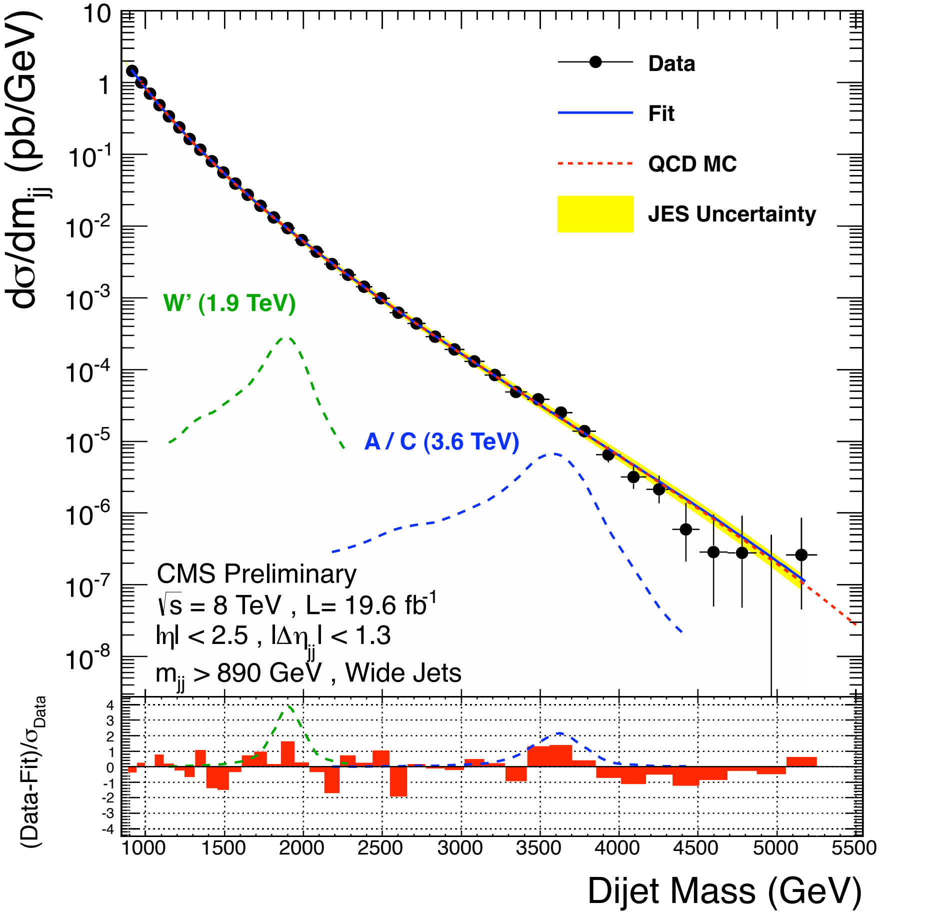

Dijet Resonances

CMS

Model	Final State	Obs. Mass Excl. [TeV]	Exp. Mass Excl. [TeV]
String Resonance (S)	qg	[1.20,5.08]	[1.20,5.00]
Excited Quark (q*)	qg	[1.20,3.50]	[1.20,3.75]
E_6 Diquark (D)	qq	[1.20,4.75]	[1.20,4.50]
Axigluon (A)/Coloron (C)	$q\bar{q}$	[1.20,3.60] + [3.90,4.08]	[1.20,3.87]
Color Octet Scalar (s8)	gg	[1.20,2.79]	[1.20,2.74]
W′ Boson (W′)	$q\bar{q}$	[1.20,2.29]	[1.20,2.28]
Z′ Boson (Z′)	$q\bar{q}$	[1.20,1.68]	[1.20,1.87]
RS Graviton (G)	$q\bar{q}$+gg	[1.20,1.58]	[1.20,1.43]

M(q*) > 3.84 (3.70) TeV [ATLAS]

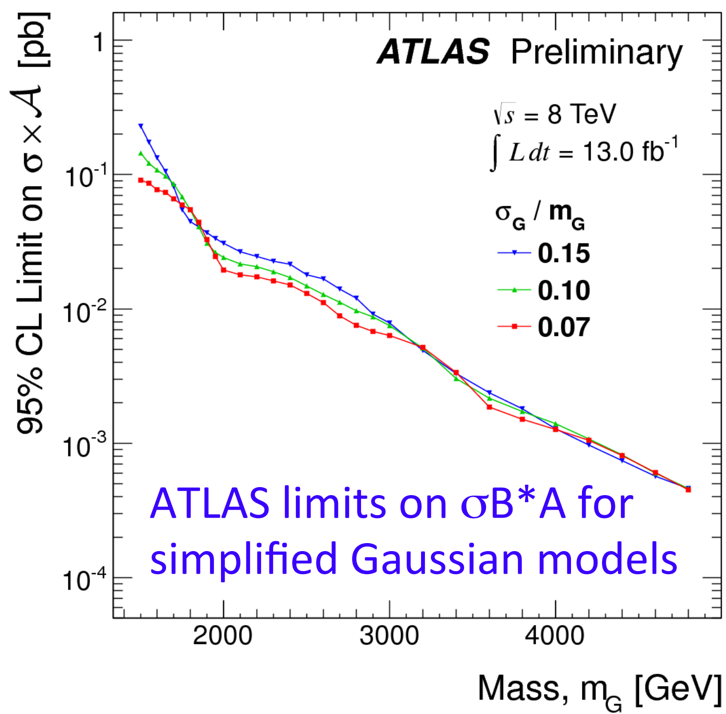

Summary

- Searches by ATLAS and CMS for new phenomena are probing the TeV scale
- The SM has proved incredibly resilient
  - Searches at the LHC have not found evidence for BSM physics…yet!
- This is only the beginning
  - Results using the full Run 1 dataset are starting to appear
  - LHC physics reach will be greatly extended by the increased beam energy and intensity expected in Run 2

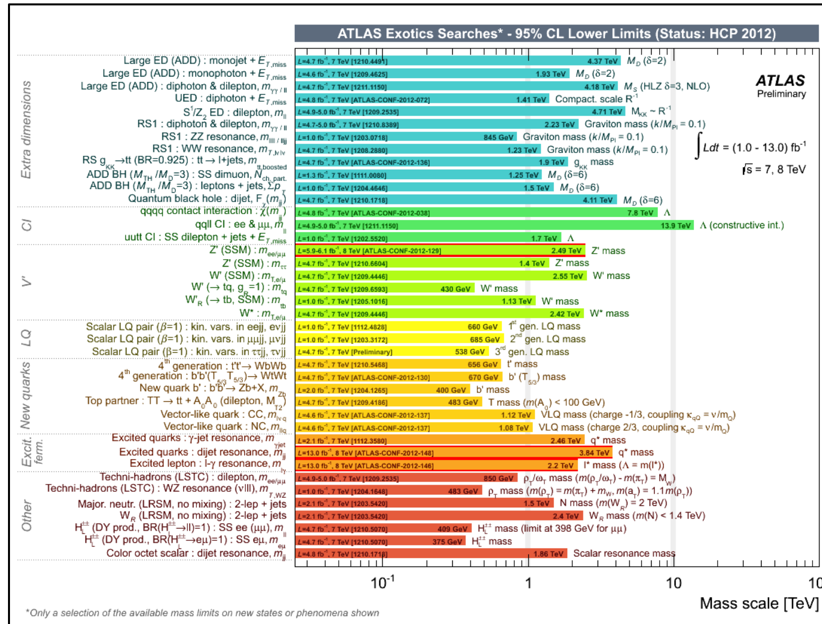

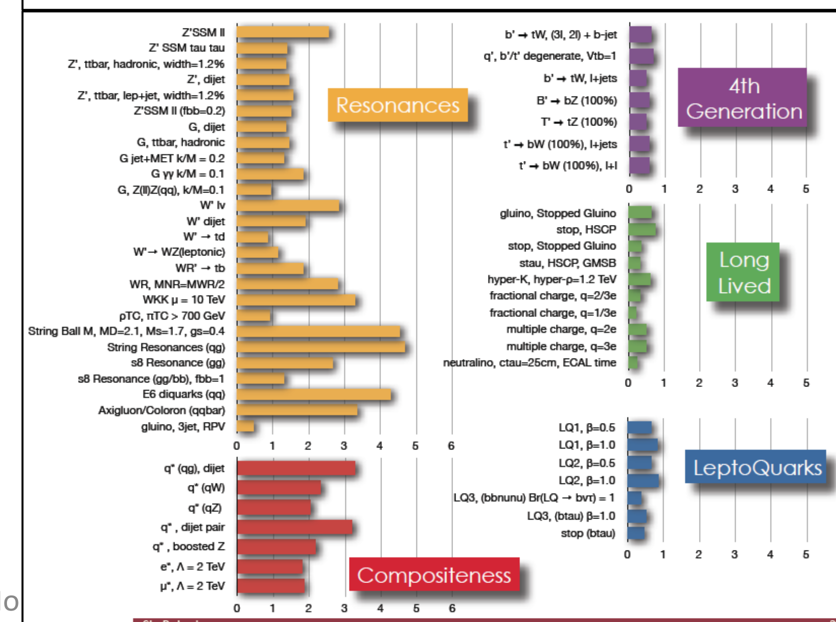

https://twiki.cern.ch/twiki/bin/view/AtlasPublic/CombinedSummaryPlots#ExoticsSummary
https://twiki.cern.ch/twiki/pub/CMSPublic/PhysicsResultsEXO/exo-limits-ichep2012.pdf

BONUS SLIDES

LHC Reach for New Physics @ 14 TeV

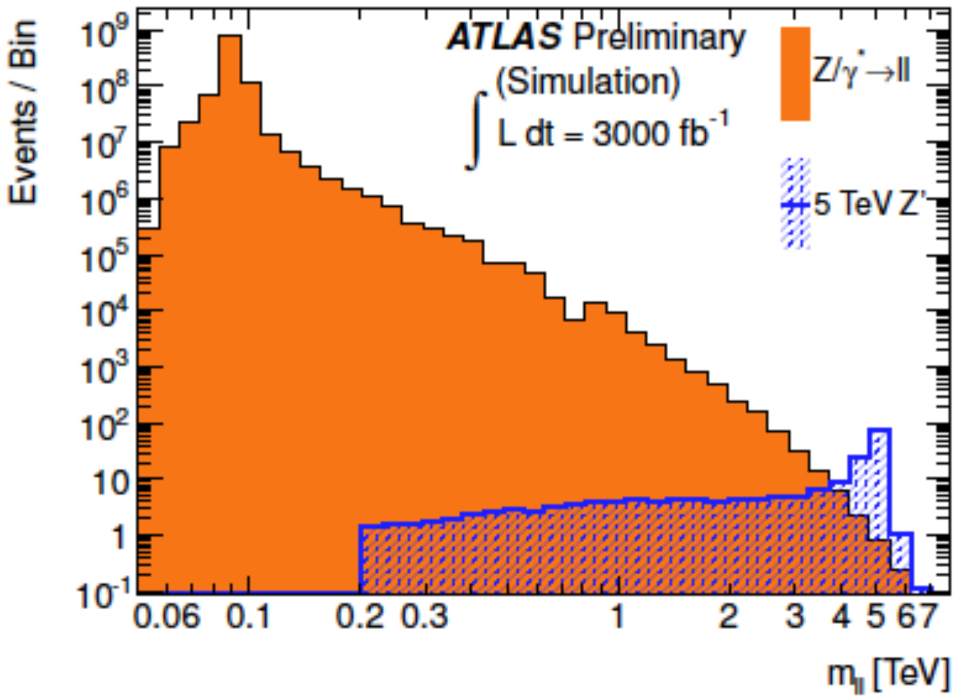

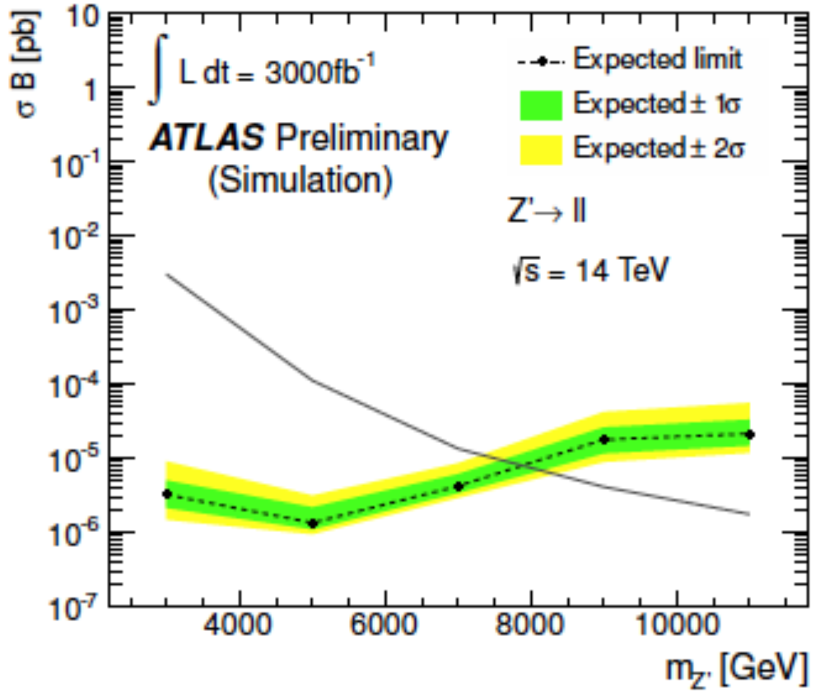

model	300 fb^{-1}	1000 fb^{-1}	3000 fb^{-1}
$Z'_{SSM} \rightarrow ee$	6.5	7.2	7.8
$Z'_{SSM} \rightarrow \mu\mu$	6.4	7.1	7.6

http://cds.cern.ch/record/1516108/files/ATL-PHYS-PUB-2013-003.pdf

High-Mass Dilepton Resonances

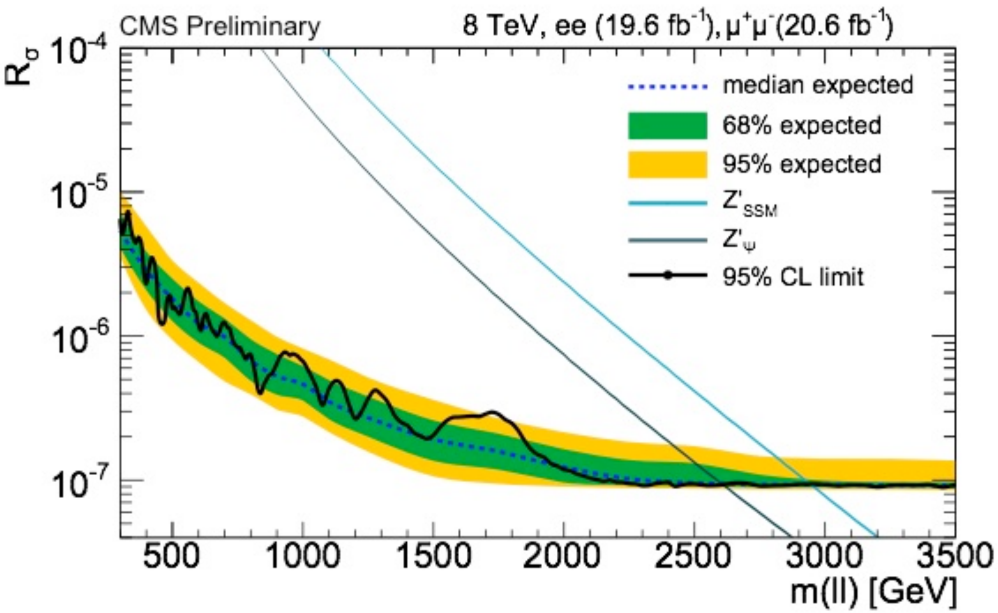

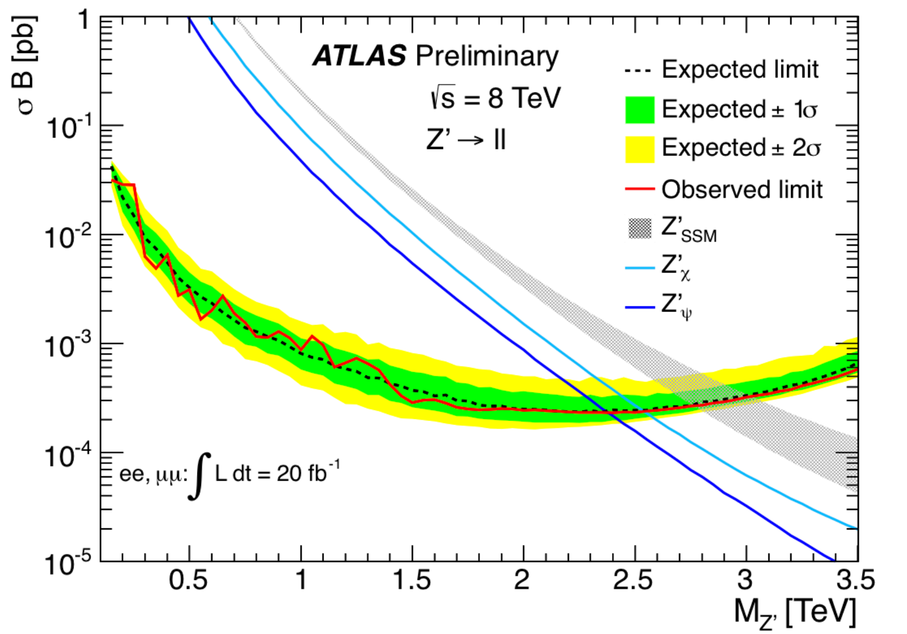

High-Mass Dilepton Resonances

Table 4: e^+e^-, $\mu^+\mu^-$ and combined 95% C.L. mass limits on Z'_{SSM}.

ATLAS

	$Z'_{\text{SSM}} \to e^+e^-$	$Z'_{\text{SSM}} \to \mu^+\mu^-$	$Z'_{\text{SSM}} \to \ell^+\ell^-$
Observed mass limit [TeV]	2.79	2.48	2.86
Expected mass limit [TeV]	2.76	2.52	2.85

Table 5: Combined mass limits at 95% C.L. on the E_6-motivated Z' models.

Model	Z'_ψ	Z'_{N}	Z'_η	Z'_I	Z'_{S}	Z'_χ
Observed mass limit [TeV]	2.38	2.39	2.44	2.42	2.47	2.54
Expected mass limit [TeV]	2.37	2.38	2.43	2.40	2.46	2.53

Table 6: e^+e^-, $\mu^+\mu^-$ and combined 95% C.L. mass limits on graviton (G^*).

	$G^* \to e^+e^-$	$G^* \to \mu^+\mu^-$	$G^* \to \ell^+\ell^-$
Observed mass limit [TeV]	2.40	2.10	2.47
Expected mass limit [TeV]	2.40	2.17	2.47

W' → Lepton + MET

Table 3: Summary of all exclusion limits in the electron and muon channels as well as their combinations. The interpretation labelled as SSM assumes no interference of W' and SM W. This interference effect is considered with opposite signs of the couplings in the model labelled as SSMO and same sign with SSMS. The reinterpretation in terms of split UED is given for two bulk mass parameters μ and the corresponding two W^2_{KK} mass limits are shown. Limits on Λ in the helicity non-conserving CI are given in the last rows.

Model	Channel	Observed limit	Expected limit
SSM	e	$m_{W'} < 3.20$TeV	$m_{W'} < 3.25$TeV
SSM	μ	$m_{W'} < 3.15$TeV	$m_{W'} < 3.10$TeV
SSM	combined	$m_{W'} < 3.35$TeV	$m_{W'} < 3.40$TeV
SSMO	e	$m_{W'} < 3.60$TeV	$m_{W'} < 3.60$TeV
SSMO	μ	$m_{W'} < 3.05$TeV	$m_{W'} < 3.30$TeV
SSMO	combined	$m_{W'} < 3.60$TeV	$m_{W'} < 3.60$TeV
SSMS	e	$m_{W'} < 3.00$TeV	$m_{W'} < 3.10$TeV
SSMS	μ	$m_{W'} < 2.80$TeV	$m_{W'} < 2.90$TeV
SSMS	combined	$m_{W'} < 3.10$TeV	$m_{W'} < 3.20$TeV
W^2_{KK}	μ=0.05 TeV, combined	$m_{W^2_{KK}} < 1.7$TeV	$m_{W^2_{KK}} < 1.7$TeV
W^2_{KK}	μ=10.0 TeV, combined	$m_{W^2_{KK}} < 3.7$TeV	$m_{W^2_{KK}} < 3.6$TeV
HNC CI	e	$\Lambda < 13.0$ TeV	$\Lambda < 13.3$ TeV
HNC CI	μ	$\Lambda < 10.9$ TeV	$\Lambda < 12.2$ TeV

Type III Seesaw Model Heavy Leptons

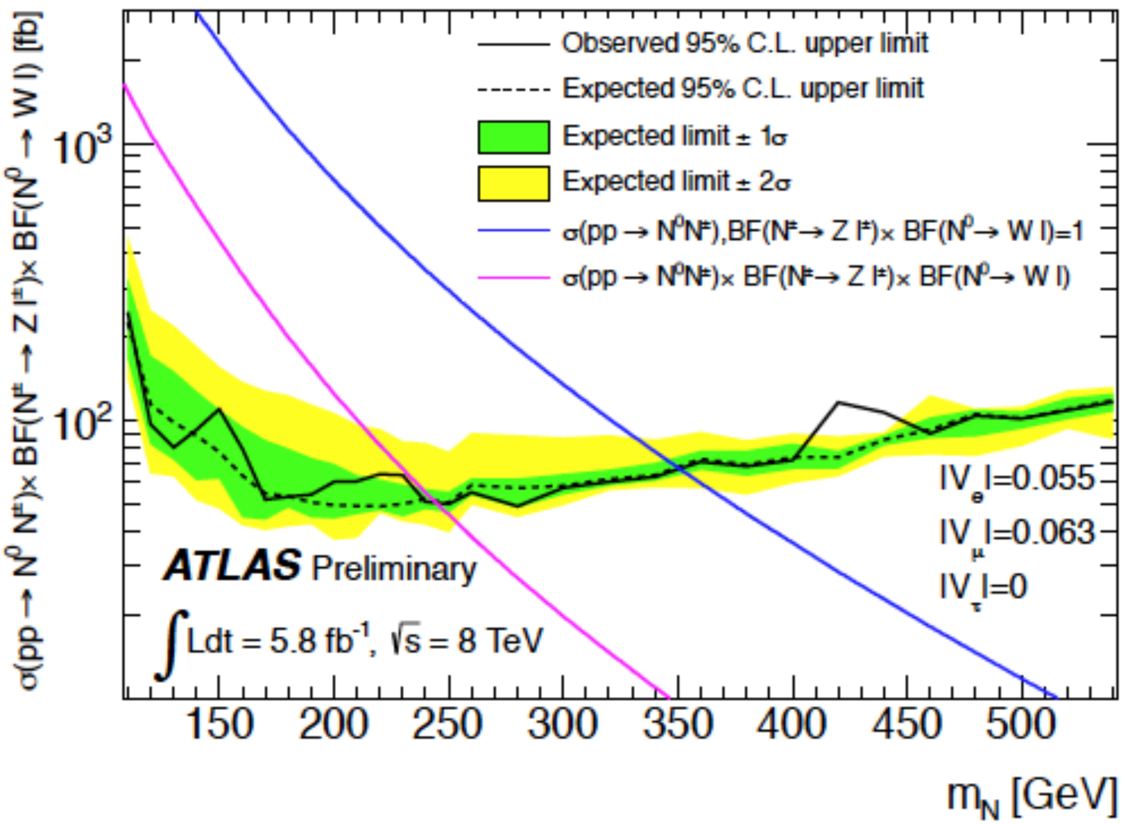

	Mass limit [GeV]	
$\mathcal{B}(N^\pm \to Z\ell^\pm)\mathcal{B}(N^0 \to W^\pm\ell^\mp)$	Expected	Observed
1.00	350	350
0.66	326	330
0.33	284	290
0.25	266	280
0.15	240	230

Resonant WZ → 3lν Production

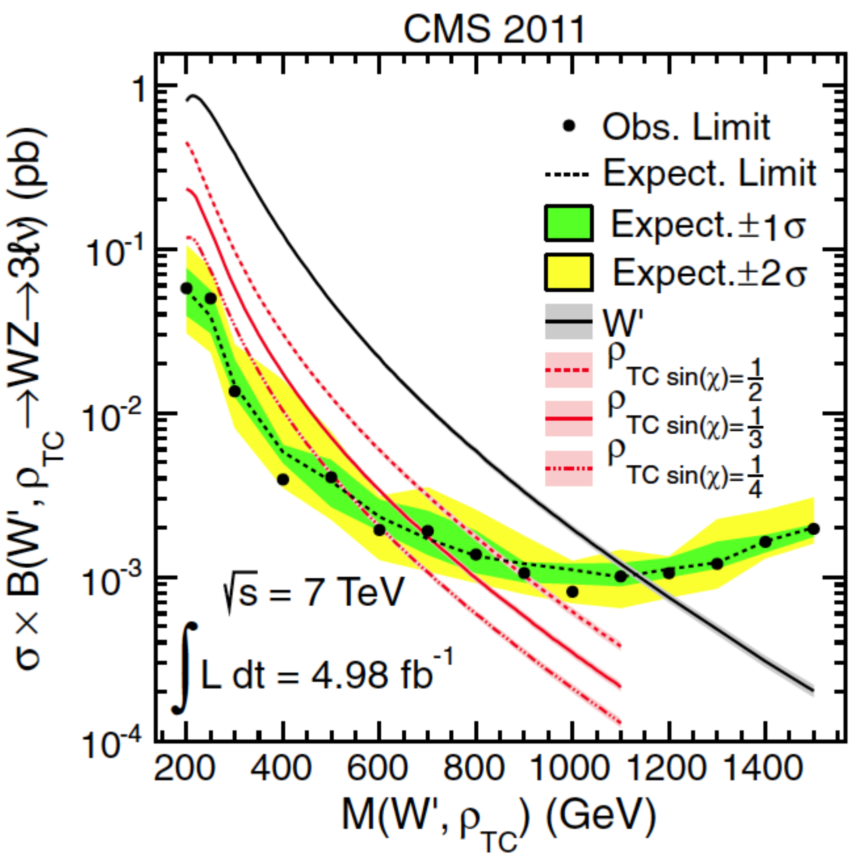

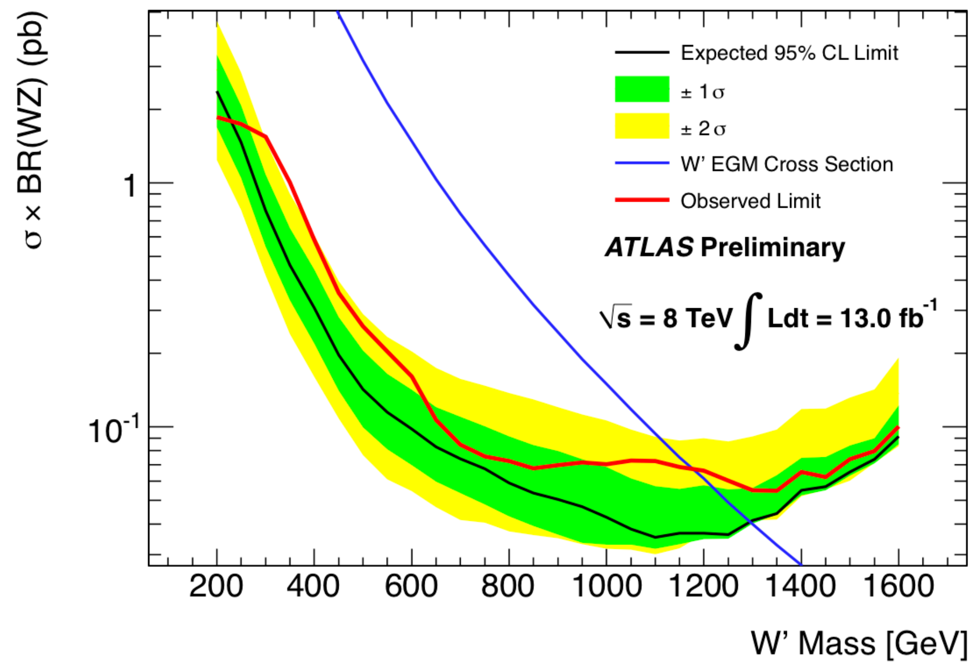

Signal	$e\nu ee$ [GeV]	$\mu\nu ee$ [GeV]	$e\nu\mu\mu$ [GeV]	$\mu\nu\mu\mu$ [GeV]	Combination [GeV]
EGM W' (expected)	1020	1030	1040	1030	1300
EGM W' (observed)	1000	1030	900	1030	1180

Resonant WZ → 3lν Production

ATLAS

	$e\nu ee$			$\mu\nu ee$			$e\nu\mu\mu$			$\mu\nu\mu\mu$			inclusive		
Region	Exp.	Obs.	p-value	Exp.	Obs.	p-value	Exp.	Obs.	p-value	Exp.	Obs.	p-value	Exp.	Obs.	p-value
$m_{WZ}>$ 350 GeV	10.9 ± 4.2	8.0	0.37	14.1 ± 3.4	17.0	0.30	17.5 ± 4.2	21.0	0.28	20.0 ± 4.0	17.0	0.36	62.5 ± 9.5	63.0	0.48
$m_{WZ}>$ 400 GeV	6.2 ± 3.0	6.0	0.60	9.2 ± 2.6	12.0	0.26	9.9 ± 3.2	13.0	0.25	12.5 ± 3.1	12.0	0.54	37.8 ± 7.1	43.0	0.29
$m_{WZ}>$ 450 GeV	4.0 ± 2.6	2.0	0.40	6.5 ± 2.2	10.0	0.18	6.2 ± 2.6	6.0	0.59	8.2 ± 2.5	9.0	0.43	25.0 ± 5.8	27.0	0.39
$m_{WZ}>$ 500 GeV	2.5 ± 2.1	2.0	0.61	4.2 ± 1.8	7.0	0.18	4.5 ± 2.2	2.0	0.28	5.7 ± 2.2	7.0	0.36	17.0 ± 4.8	18.0	0.43
$m_{WZ}>$ 550 GeV	1.7 ± 1.7	1.0	0.60	3.1 ± 1.5	5.0	0.23	2.9 ± 1.8	0.0	0.15	4.0 ± 1.8	5.0	0.36	11.6 ± 4.2	11.0	0.54
$m_{WZ}>$ 600 GeV	1.1 ± 1.1	1.0	0.72	2.3 ± 1.3	3.0	0.38	2.1 ± 1.1	0.0	0.18	2.9 ± 1.5	2.0	0.50	8.5 ± 3.3	6.0	0.37
$m_{WZ}>$ 650 GeV	0.7 ± 0.6	1.0	0.45	1.4 ± 1.0	2.0	0.36	1.7 ± 0.9	0.0	0.26	2.5 ± 1.4	2.0	0.59	6.2 ± 2.3	5.0	0.46
$m_{WZ}>$ 700 GeV	0.4 ± 0.4	1.0	0.30	0.9 ± 0.8	2.0	0.23	1.2 ± 0.7	0.0	0.39	1.9 ± 1.2	2.0	0.49	4.4 ± 1.9	5.0	0.42
$m_{WZ}>$ 750 GeV	0.3 ± 0.3	1.0	0.24	0.7 ± 0.6	2.0	0.17	0.9 ± 0.6	0.0	0.48	1.4 ± 1.0	2.0	0.37	3.3 ± 1.5	5.0	0.26
$m_{WZ}>$ 800 GeV	0.3 ± 0.3	1.0	0.21	0.5 ± 0.5	1.0	0.36	0.6 ± 0.5	0.0	0.59	1.2 ± 0.9	1.0	0.70	2.6 ± 1.3	3.0	0.45
$m_{WZ}>$ 850 GeV	0.1 ± 0.1	1.0	0.11	0.5 ± 0.5	1.0	0.32	0.4 ± 0.4	0.0	0.70	0.9 ± 0.8	0.0	0.50	1.9 ± 1.1	2.0	0.51
$m_{WZ}>$ 900 GeV	0.1 ± 0.1	1.0	0.08	0.3 ± 0.3	1.0	0.23	0.3 ± 0.3	0.0	0.79	0.8 ± 0.7	0.0	0.53	1.5 ± 0.9	2.0	0.39

Table 2: The observed and expected numbers of events in different m_{WZ} regions. The p-value, which is defined as the probability for the expected number of events to fluctuate to the observed number of events or beyond, assuming a Poisson distribution of the expected number of events, is also shown. The relative uncertainties on the expected background were calculated in a conservative fashion by symmetrizing them in each bin and correlating them between different bins. This together with the statistical fluctuations of each individual channel produces the relative uncertainties shown above.

Resonant WZ → 3lν Production

ATLAS

Sample	*eνee* Channel	*μνee* Channel	*eνμμ* Channel	*μνμμ* Channel	Sum
Backgrounds:					
WZ	$39.1 \pm 1.2 \pm 4.0$	$52.0 \pm 1.4 \pm 5.2$	$60.2 \pm 1.4 \pm 5.8$	$81.5 \pm 1.6 \pm 7.7$	$233 \pm 3 \pm 22$
ZZ	$3.7 \pm 0.1 \pm 0.3$	$3.3 \pm 0.1 \pm 0.2$	$3.6 \pm 0.1 \pm 0.3$	$4.4 \pm 0.1 \pm 0.3$	$15.0 \pm 0.2 \pm 0.9$
$Z\gamma$	$2.4 \pm 1.0 \pm 0.9$	*negl.*	$6.0 \pm 1.8 \pm 0.8$	*negl.*	$8.4 \pm 2.1 \pm 1.2$
Fake Background (data-driven)	$4.0 \pm 1.0^{+1.7}_{-1.6}$	$6.6 \pm 1.1^{+2.5}_{-2.3}$	$11.0 \pm 1.7^{+5.2}_{-4.7}$	$8.0 \pm 1.2^{+3.2}_{-3.1}$	$29.6 \pm 2.6^{+6.8}_{-6.3}$
Sum of Backgrounds	$49.2 \pm 1.9 \pm 4.4$	$61.9 \pm 1.8 \pm 5.8$	$80.8 \pm 2.8 \pm 7.8$	$93.9 \pm 2.0 \pm 8.3$	$286 \pm 4 \pm 24$
Data	55	73	98	98	324
Signals:					
$W' \to WZ$ ($M(W')$ = 800 GeV)	7.8 ± 0.2	8.5 ± 0.2	9.0 ± 0.2	10.1 ± 0.2	35.4 ± 0.4
$W' \to WZ$ ($M(W')$ = 1000 GeV)	3.1 ± 0.1	3.3 ± 0.1	3.5 ± 0.1	3.5 ± 0.1	13.4 ± 0.2
$W' \to WZ$ ($M(W')$ = 1200 GeV)	1.3 ± 0.1	1.3 ± 0.1	1.3 ± 0.1	1.4 ± 0.1	5.3 ± 0.1
$\rho_T \to WZ$ ($M(\rho_T)$ = 400 GeV)	14.2 ± 0.7	17.8 ± 0.7	22.3 ± 0.8	25.0 ± 0.8	79.3 ± 1.6
$\rho_T \to WZ$ ($M(\rho_T)$ = 600 GeV)	4.9 ± 0.2	5.8 ± 0.2	6.7 ± 0.2	7.3 ± 0.2	24.7 ± 0.4
$\rho_T \to WZ$ ($M(\rho_T)$ = 800 GeV)	2.0 ± 0.1	1.9 ± 0.1	2.3 ± 0.1	2.6 ± 0.1	8.8 ± 0.2

Table 6: The estimated background yields, the observed number of data events, and the predicted signal yield after applying the basic signal selection cuts. No selection on the *WZ* invariant mass is applied.

Resonant ZZ Production

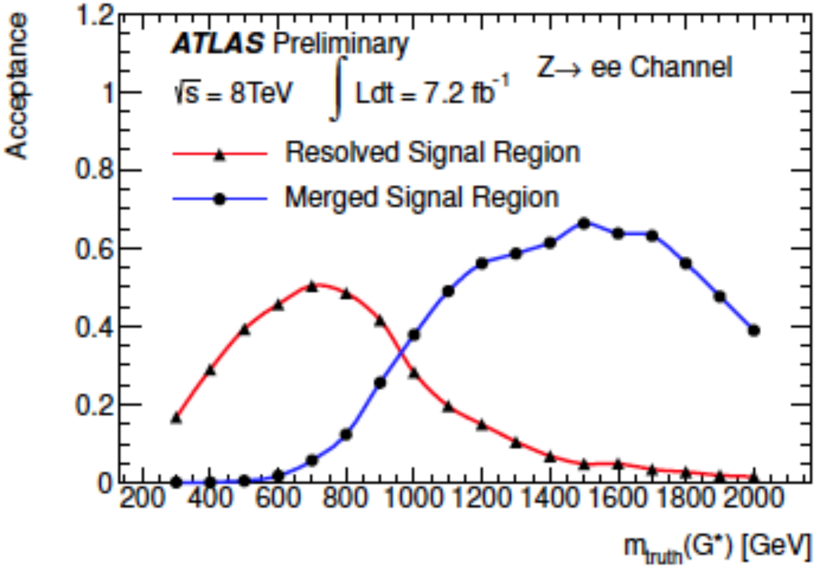

(a)

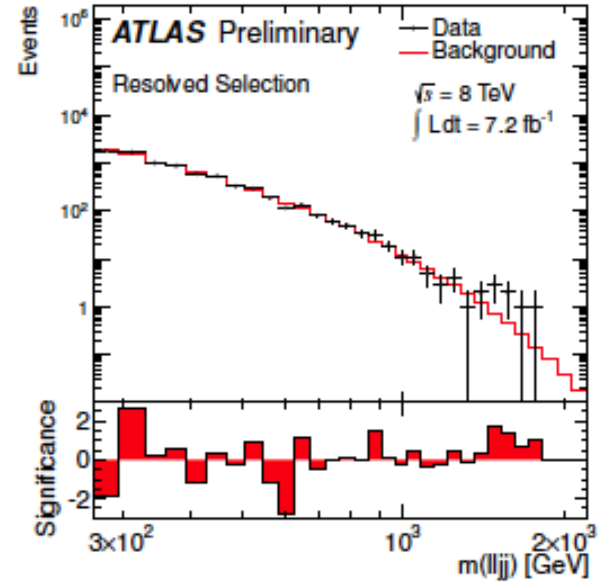

(a)

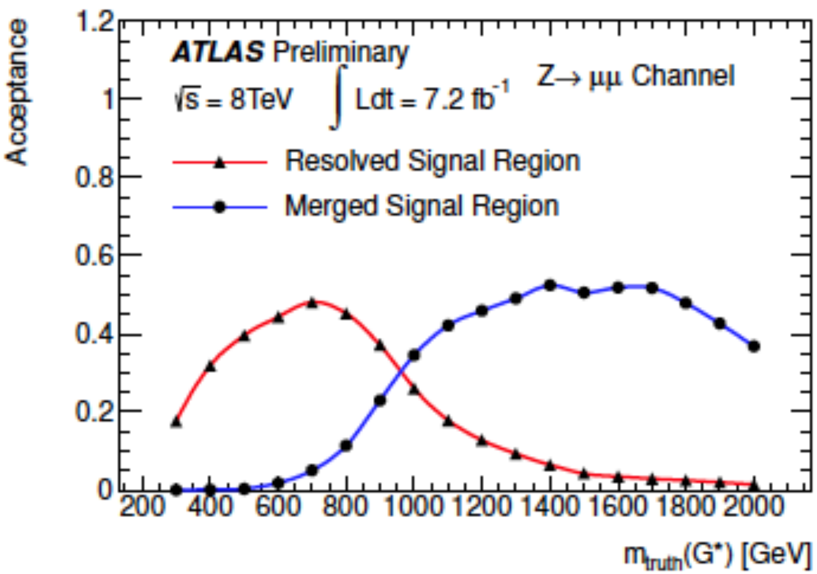

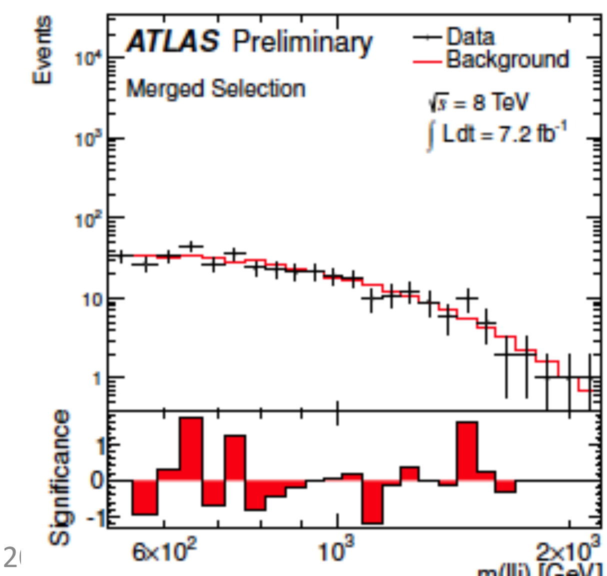

Search for Dijet Resonances

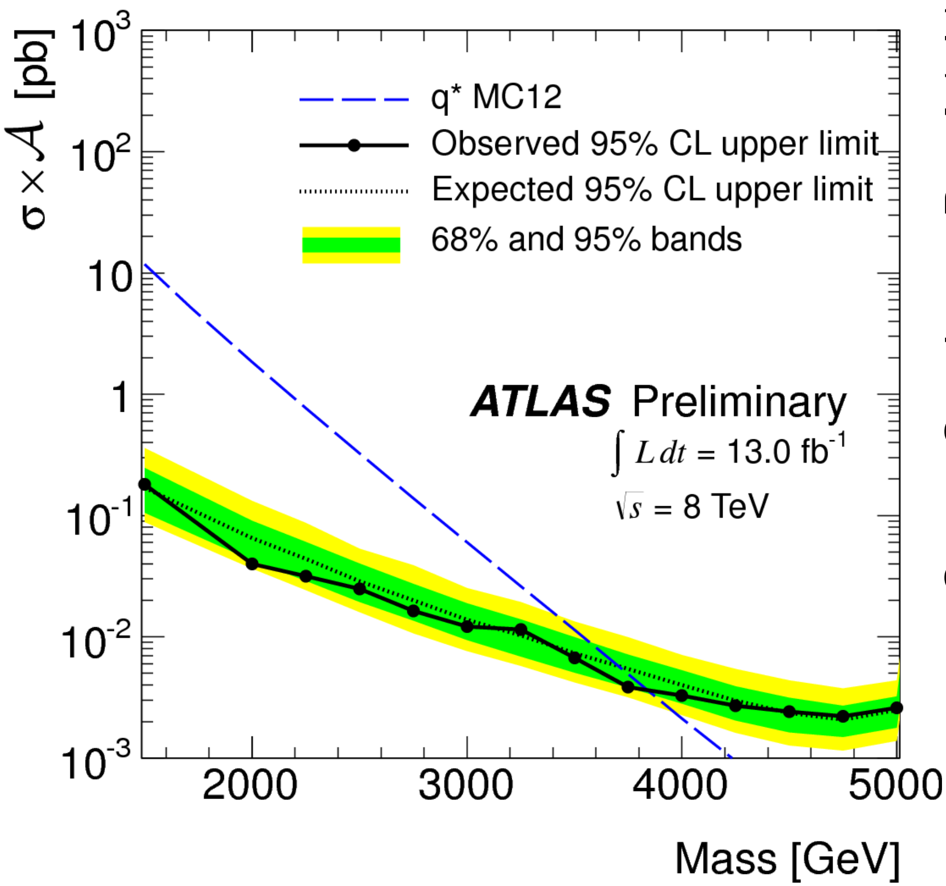

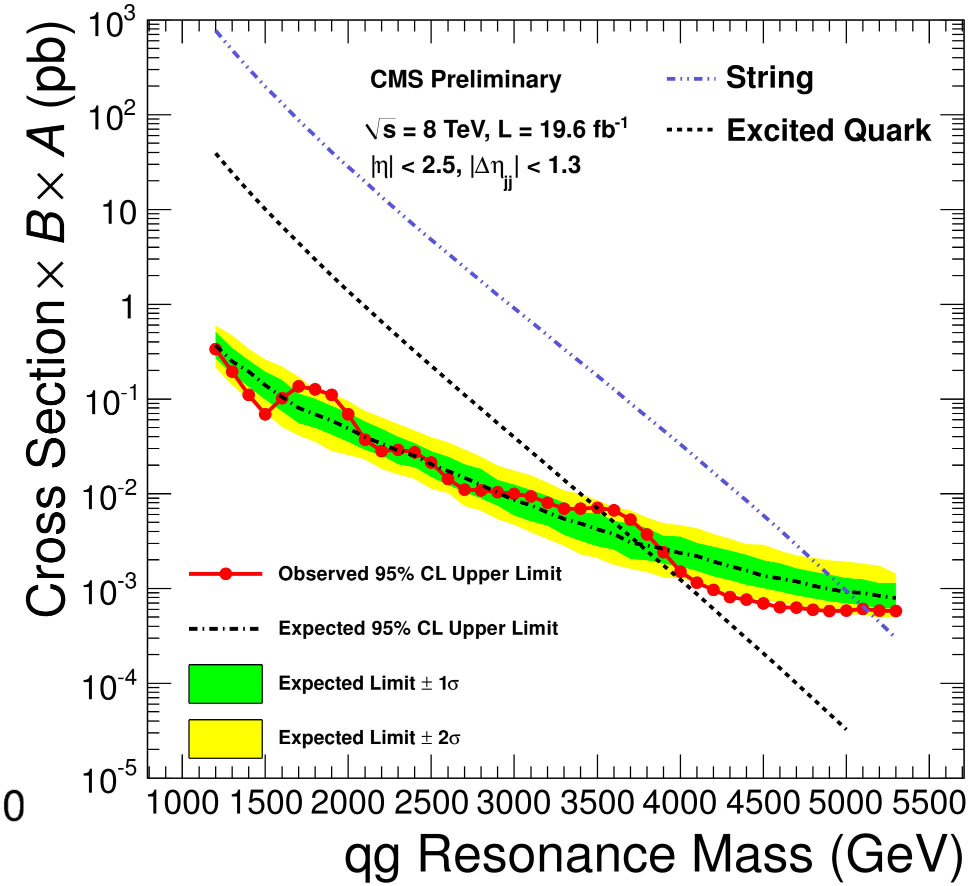

Search for Dijet Resonances